EARTH'S CRYOSPHERE
SCIENTIFIC JOURNAL

Earth's Cryosphere, 2022, vol. XXVI, No. 5, pp. 25–34

CRYOGENIC PHENOMENA IN SEAS AND OCEANS

FREQUENCY OF OCCURRENCE OF FAST ICE CALCULATED FROM POLYGONS OF DIGITIZED ICE CHARTS USING THE EXAMPLE OF THE KARA SEA

R.I. May[1,2,*], K.R. Ganieva[1], A.G. Topaj[3], A.V. Yulin[4]

[1] *St. Petersburg State University, Department of Oceanology, Universitetskaya Emb. 7/9, St. Petersburg, 199034 Russia*
[2] *Krylov State Research Center, Moskovskoe shosse 44, St. Petersburg, 196158 Russia*
[3] *LLC "Bureau Hyperborea", Kavalergardskaya St. 6A, St. Petersburg, 191015 Russia*
[4] *Arctic and Antarctic Research Institute, Beringa St. 38, St. Petersburg, 199397 Russia*

**Corresponding author; e-mail: rimay@mail.ru*

Many elements of the natural environment are areal objects that change their position and shape at all scales of variability. For sea ice, such elements can be fast ice, drifting ice, polynyas, ice massifs, and boundaries of multi-year ice. In other earth sciences, these are the boundaries of glaciers, permafrost, snow cover, forest zone, and various isolines of meteorological and oceanological fields (isotherms, isobars, etc.). To analyze such objects, one can usually use approximations in the form of a grid area (rasterization) or a system of sections. In this article, we suggest a direct analysis of these objects based on operations with vector polygons. An efficient algorithm for calculating the probability (frequency of occurrence) of an unlimited number of polygons has been developed and tested. A criterion for selecting one of the real edges of a polygon as an analogue of the isoline of the probability of intersections of polygons is proposed. The developed method has been tested using data on the fast ice of the Kara Sea taken from the digital ice charts developed by the Arctic and Antarctic Research Institute for 1998–2020. As a result, the charts of fast ice probability for the cold season of each year and for a given time of the year for the entire considered period have been obtained. Based on these data, the operational characteristics of fast ice have been estimated, and a tendency for a decrease in the area of fast ice during the considered period has been revealed. For the beginning of May (the period of the maximum development of fast ice), analogues from factual observations characterizing extreme, median, and quartile probability isolines of fast ice occurrence have been found.

Keywords: *fast ice, sea ice, Kara Sea, analysis of polygons.*

Recommended citation: May R.I., Ganieva K.R., Topaj A.G., Yulin A.V., 2022. Frequency of occurrence of fast ice calculated from polygons of digitized ice charts using the example of the Kara Sea. *Earth's Cryosphere* **26** (5), 25–34.

INTRODUCTION

The fast ice of the Arctic seas (fixed ice along the coastline) is a unique ice formation that is constantly formed during the cold season in the coastal zone of the coast of the mainland and the islands. The presence of fast ice is a characteristic feature of the ice regime of the Arctic seas in the winter season [*Vize, 1944, 1948; Zubov, 1944*]. According to the definition [*Volkov, 1981; WMO No. 259, 2014; Atlas..., 2018*], fast ice is considered to be sea ice that forms and remains motionless along the coast, where it is attached to the shore, ice wall, ice barrier, between shoals, or between grounded ice hummocks. Fast ice can form naturally from salt water or when floating ice of any age category freezes to the shore or to the already existing fast ice.

As a rule, fast ice has the maximum thickness among ice of the same age due to its long and calm growth [*Gudkovich et al., 1972; Gorbunov et al., 1983*]. Fast ice radically changes the characteristics of the hydrological regime of the occupied water area. Fast ice (as opposed to drifting ice) is one of the reasons for the seasonal variability of tide characteristics. The circulation of water under fast ice differs from the circulation of water under drifting ice. The fast ice boundary can be an area of intense hummock formation during ice pressure drift. Vice versa, during offshore winds, polynyas with special hydrological and thermal balance conditions are formed near the fast ice boundaries [*Gordienko, 1971; Karelin, Karklin, 2012*]. Fast ice is important from a practical perspective: on the one hand, it can become an obstacle to navigation, on the other hand, fixed ice can serve as a temporary berth for unloading cargo at an unequipped shore. Polynyas formed near the fast ice are, most often, the easiest areas for Arctic navigation. The channel laid in the fast ice retains its position and is used during the entire navigation period.

The evaluation of fast ice regime characteristics along the given sections was carried out in [*Dmitrenko et al., 1999; Karelin, Karklin, 2012; Arkhipov et al.,*

2017]. The Arctic and Antarctic Research Institute (AARI) uses standard alignments that run perpendicular to the coastline. The distance between the sections varies from 50 to 150 km; the Kara Sea has only 28 standard sections [*Karelin, Karklin, 2012*]. Obviously, the accuracy of the fast ice description depends on the number of selected sections. At large distances between the sections, the obtained statistical characteristics are polygonal objects with a rough spatial resolution. The paper [*Pavlova et al., 2019*] gives a quantitative estimate of the error in determining the maximum fast ice in the Kara Sea based on data from standard AARI sites: the maximum error in the fast ice width is ~30–40 km.

Increasing the gate frequency can offset this error to some extent. For the coast of Alaska, sections were drawn along the points located on the coast and a line 150 km away from the coast [*Mahoney et al., 2007, 2014*]. The alignment points on the sea line were spaced apart at 1 km from one another and connected to the nearest points on the coast. Based on the composition of various radar satellite images, the coordinates of the fast ice edge were determined. Thus, a frequent alignment was used for automatic delineation of the boundaries of fast ice and the determination of some statistical characteristics of its distribution along the sections [*Mahoney et al., 2007, 2014*].

Even with a high frequency of alignments, this method contains uncertainties: with a winding coastline (bays, gulfs, capes, peninsulas, islands), the alignments perpendicular to the coast can intersect, lie entirely within the fast ice fields, cross the edges of the fast ice of opposite coasts, etc.

Another method for studying the regime characteristics of fast ice is based on the use of grid areas, the nodes of which contain a sign of the presence or absence of fast ice. This method was used in [*Divine et al., 2004; Mahoney et al., 2007, 2014; Galley et al., 2012; Yu et al., 2014; Selyuzhenok et al., 2015; Li et al., 2020*]. The sum of signs of the presence or absence of fast ice in each cell of the grid area, related to the total number of analyzed fields of fast ice, allows us to estimate the probability of the presence of fast ice in the cell. In this case, in grid methods, the results of analysis depend on the spatial step. The problem of fast ice approximation by a grid area was raised in [*Yu et al., 2014; Pavlova et al., 2019*].

Obviously, the smaller the spatial grid step, the more accurate the approximation. However, acceptable spatial grid steps require significant computational resources. In studies of the regime characteristics of fast ice, grids with spatial steps from 100 m [*Mahoney et al., 2007, 2014*] to 12.5 km [*Divine et al., 2004; Yu et al., 2014*] are used. Thus, the analysis of fast ice variability can be based on the gate and grid methods. Modern information on ice is represented by vectorized polygons that describe areal objects (fast ice, ice zones, polynyas, leads) in the form of a sequence of coordinates of boundary points. At the same time, statistical analysis of data in the form of lines (curves, functions) is fundamentally possible [*Ramsay, Silverman, 2005*].

MATERIALS AND METHODS

Electronic ice charts

Special SIGRID formats have been developed for the storage and dissemination of ice information, allowing the storage of multidimensional ice cover data. The first two versions of the format were based on the matrix principle of information storage. In 1995, the AARI developed the SIGRID-3 format, which allows storing vector information about the ice cover in the form of polygons that outline certain zones with the same ice parameters. This vector format is most suitable for describing ice zones in general and fast ice, in particular. To store polygons of ice zones in the SIGRID-3 format, the geographic information system file structure developed by ESRI is used. The SIGRID-3 format has been adopted by the World Meteorological Organization as the main format for the storage and dissemination of ice information. This format is used by major sea ice research centers.

This article describes the results of the analysis of ice information provided by the AARI through the World Data Center–Sea Ice (WDC-SI) [*http://wdc.aari.ru/datasets*]. The information covers the interval from 1997 to the present time with weekly time step. The AARI ice charts presented on the WDC-SI website were created based on the analysis of satellite information in various ranges of the electromagnetic spectrum by ice experts. An ice expert determines ice zones based on his experience, knowledge of the regime characteristics of the ice cover in a given area, and on constant monitoring of changes in the ice situation. Each ice expert specializes in a separate water area, so AARI provides ice charts separately for 12 Arctic and freezing seas of Russia [*Afanasyeva et al., 2019*]. This paper presents calculations of the regime characteristics of the appearance of fast ice using the example of the Kara Sea as a water area where year-round navigation of ships is carried out.

In each electronic ice chart, coordinates of the fast ice boundaries are given with due account for the ice zone. Separate fast ice areas observed in a given time are combined into one landfast ice polygon. Since AARI ice charts are created manually by experts, in some cases, objective and subjective errors may occur. At the first stage, all landfast ice polygons are visually checked for such errors. Ice charts that do not display information about fast ice in some separate part of the water area are considered unsuitable for analysis (December 22, 1999; June 5, 2003; April 29, 2014; December 25, 2018). In some cases,

either fast ice is completely absent (October 30, 2003; February 27, 2018), or the displayed fast ice polygon differs significantly from the information of ice charts adjacent in time (August 12, 2003). In addition, on some ice charts, the fast ice polygon is artificially cut off in the Gulf of Ob and the Yenisei Bay. The missing sections of the landfast ice polygons in the Gulf of Ob and the Yenisei Bay are restored to avoid errors in the calculation of areas during the analysis due to artificial distortions of the ice zones.

Operations with vector polygons

Operations with polygonal objects can be described with mathematical symbols from the algebra of sets: union of polygons ($A \cup B$), subtraction of polygons (A\B) and intersection of polygons ($A \cap B$) (Fig. 1). Based on these three steps, it is possible to create algorithms for calculating the repeatability (probability) of polygon intersections. Consider a sample of N polygons P_n, $n = 1, ..., N$, for which we will build probabilistic intersection polygons – an analogue of constructing a histogram or an empirical probability distribution for scalar quantities. The composition of this sample is determined by the semantics of the problem under consideration. For example, it can include all polygons for a limited period of a calendar year (landfast ice distribution in April) or the entire ice season. The union of all landfast ice polygons P_n will give one vast polygon, maximum in area and coverage, where landfast ice was noted at least once. This polygon $Q_{1/N}$ will correspond to the area, where the probability of finding landfast ice is greater than or equal to $1/N$:

$$Q_{1/N} \geq \bigcup_{n=1}^{N} P_n.$$

Meanwhile, the intersection of all sample polygons forms a set of points where landfast ice is observed for all considered ice charts; in other words, this is the area where the probability of finding landfast ice is N/N, that is, one:

$$Q_1 = Q_{N/N} = \bigcap_{n=1}^{N} P_n.$$

Along with these extreme cases, it is of interest to determine the areas occupied by landfast ice with any intermediate probability n/N, where $n = 1, ..., N$. The most obvious algorithm for calculating such polygons of probabilities $Q_{n/N}$ is as follows. It is necessary to consider sequentially all subsets of the complete sample, consisting of exactly n polygons without repetitions and without taking into account permutations. For each of these subsamples Ω_k, we find the intersection of its component polygons and all these intersections merge:

$$Q_{n/N} = \bigcup_{k=1}^{C_n^N} \left(\bigcap_{\Omega_k} P_i,\ i \in \Omega_k \right), \qquad (1)$$

where $C_n^N = \dfrac{N!}{n!(N-n)!}$ is the number of combinations.

Unfortunately, the direct sequence of operations according to formula (1) often cannot be technically implemented due to exponentially increasing computational complexity. So, for the size of the initial sample of 22 polygons and the calculation of the "median" polygon of intersections, i.e., for $n = 11$, the number of analyzed subsamples is equal to the number of combinations from 22 to 11, which is 705,432 variants. Of course, performing several operations with vector polygons is difficult.

Perhaps this feature of the most obvious algorithm (1) explains the fact that up to now, no analysis of polygons has been carried out directly, without an intermediate raster (grid) or gate approximation. To solve this problem, the authors proposed, implemented, and tested an algorithm for recursively recalculating the entire set of probabilistic intersection polygons while successively adding new initial polygons to the sample. We can say that this algorithm is analogous to adaptive statistical estimation algorithms. Indeed, let at the $(n-1)$-th step of our algorithm, i.e., for $n-1$ already processed polygons, we know the probabilistic polygons of the intersection $R_{k/N}$, where each such polygon is a set of points falling strictly into k initial polygons (in contrast to the polygons of the intersection Q, for which the membership condition is formulated as "no less than in k initial polygons"). Then, when a new initial polygon P_n is introduced into consideration, all these polygons are recalculated at a new step of the algorithm according to a simple rule:

$$R_{k/N}^{n} = \left(R_{k-1/N}^{n-1} \cap P_n \right) \cup \left(R_{k/N}^{n-1} \setminus P_n \right);$$
$$R_{k/N}^{0} = \varnothing,\ k = 1,...,N. \qquad (2)$$

Formula (2) demonstrates how a set of points forming the k-th set of intersections of the initial

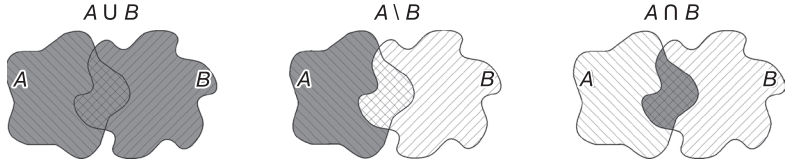

Fig. 1. Operations with vector polygons.

polygons is created when a new initial polygon appears. These points coincide with the points for the corresponding (k–1)-set at the previous step, which fall into the new polygon, and the points for the corresponding k-set at the previous step, which do not fall into the new polygon.

In the meantime, the polygons of intersections of the cumulative probability $Q_{n/N}$ that are of interest to us can always be calculated using the formula:

$$Q_{n/N} = \bigcup_{k=1}^{n} R_{k/N}. \quad (3)$$

The algorithm described by formulas (2) and (3) allows quick recursive calculation of the polygon intersection probability for an unlimited number of polygons P_n, since the computational complexity of the algorithm grows with an increase in the number of polygons only in a quadratic dependence.

The spatial slice of the obtained intersection frequency field, drawn orthogonally to the coastline and the polygons of probability Q_p, will outwardly resemble the empirical function of the spatial distribution of the probability value, where the distance is plotted along the abscissa axis, and the probability values varying from 0 in the seaward part to 1 at the coast are plotted along the ordinate. Thus, it is possible to find correspondences between the considered method of vector polygon analysis and the gate method. At the same time, it is possible that along such a cut there will be local decreases in probabilities associated with the influence of local conditions (the influence of landfast ice located near individual islands, prominent elements of the coastline, ice hummocks, etc.). Such effects inherent in the gate method are associated with the choice of the position and direction of the slices.

In the accepted notation, the analogue of the interquartile distance will be the Q_{IQR} polygon, which can be calculated as the difference between the polygons $Q_{p=0.25}$ and $Q_{p=0.75}$:

$$Q_{IQR} = Q_{p=0.75} \setminus Q_{p=0.25}. \quad (4)$$

It should be noted that the obtained "probabilistic" polygons of finding landfast ice Q_p will never exactly coincide with any of the actually observed landfast ice edges P_n. The probability isolines obtained during vector operations will be a broken line composed of fragments of landfast ice edges for different years or dates. Therefore, it is of interest to be able to replace the obtained "virtual" isoline with its close analogue from the real world. To select one of the observed landfast ice edges P_n closest to Q_p, one can use the concept of "functional data depth" [*Lopez-Pintado, Romo, 2009*]. In functional data analysis, the "depth" function determines how "deep" a point or curve is in the selected data cloud in Euclidean space, that is, how close it is to an implicitly defined center that has a maximum "depth". The authors propose using the condition $S(D_n)$ = min as a criterion for the "depth" of the landfast ice line, i.e., its correspondence to the obtained "virtual" standard, where the chosen proximity norm $S(D_n)$ is the area of polygon D_n, which is determined from the equation

$$D_n = \left(Q_p \setminus P_n\right) \cup \left(P_n \setminus Q_p\right).$$

From the entire set of observed landfast ice polygons P_n, the one for which the polygon area D_n is minimal is selected. A similar criterion is used in the least squares method: the minimum of the sum of squares of the difference between the data and the approximating function has the geometric meaning of the minimum of the area between the measured values and the function.

The algorithm for calculating the probability of polygon intersections described above was implemented in the MatLab language as a set of programs and functions, the files of which can be found in the public domain at [*https://www.mathworks.com/matlabcentral/fileexchange/99879-probability-of-polygon-sintersection*].

RESULTS AND DISCUSSION

The AARI ice charts are provided with weekly discreteness, therefore, for the analysis of landfast ice polygons, the authors used ten-day periods; each month was divided into three such periods. From the entire data array, ice charts closest in time to the central day of the ten-day period were selected. Thus, as such central dates, the authors chose days 5, 15, and 25 of each month. Taking into account that ice charts are created from a series of satellite images covering several days, it can be assumed that the maximum deviations of three days for the dates of a weekly and ten-day discreteness will not greatly affect the results of the analysis.

Using the method described above for estimating the probability of crossing polygons, it is possible to determine the operational characteristics of the occurrence of landfast ice. Depending on the period of time, for which the data array is analyzed, it is possible to estimate the seasonal or interannual variability of landfast ice frequency.

Analysis of data for one cold season will show the repeatability of the landfast ice position for a given year. A comparison of annual charts of landfast ice position frequency for several years will reveal interannual variability. As an example, polygons of landfast ice position probability during one cycle of formation and destruction (October–July) for 2000, 2005, 2010, 2015, and 2020 are given (Fig. 2). A series of charts shows a trend towards a decrease in the area occupied by landfast ice. For 1999–2005, the landfast ice of Sergey Kirov Islands (77°15′ N, 91° E) and of Voronin Island (77°15′ N, 91° E) for most of the con-

sidered period (October–July) are located inside a vast landfast ice field connected to the mainland. As seen in Fig. 2, the probability of finding landfast ice between these islands and the Taimyr Peninsula in 2000 and 2005 is 0.6–0.8, i.e., landfast ice occurs for 15–21 ten-day periods out of 27. Similar probability values are observed for other years in the interval from 1998 to 2005, except for 2002, when landfast ice connected to the mainland was observed only during 2–3 ten-day periods out of 27 decades (probability about 0.1). From 2008 to 2020, a different picture is noted: landfast ice of Sergey Kirov and Voronin islands was connected with the mainland landfast ice in less than 11 ten-day periods out of 27 (probability less than 0.41) (Fig. 2). The exception is 2013, when the probability of landfast ice occurrence between these islands and the Taimyr Peninsula was 0.66 (17 ten-day periods out of 27), while in 2012, 2016, and 2017 landfast ices of the islands of Sergei Kirov and Voronin remained isolated from the mainland landfast ice. A similar trend (a decrease in the probability of landfast ice occurrence over the considered period) was noted for the Gulfs of Ob and Gydan and the Yenisei Bay (Fig. 2).

In addition to a qualitative description of the interannual variability, the obtained polygons of the probabilities of the landfast ice position can give some quantitative characteristics: the area or linear width of the landfast ice. For example, the representation of the probability quantiles of the occurrence of landfast ice in the form of polygons will allow one to find the area occupied by the quantile of a given probability. Now, to study the interannual and climatic variability of landfast ice distribution, time series of the maximum or average area of landfast ice per year are used. The time series of areas occupied by quantiles of different probabilities may make it possible to reveal hidden patterns of interannual and climatic variability of landfast ice.

Another frequently used method for calculating the regime characteristics of the state of natural parameters subjected to seasonal variability is to analyze data separated by one year. For example, let us determine the probability of the appearance of landfast ice in the first ten days of May for the entire time of observations. The choice of the first ten days of May is because at this time the maximum landfast ice areas in the Kara Sea are observed.

Landfast ice with a probability of 1 (minimum development) is observed in the Taz Bay, the southern part of the Gulf of Ob, the Gydan Bay, the Yenisei Bay in the form of a narrow strip near the Yamal coast of the Baydaratskaya Bay, in the Malygin Strait separating Belyi Island from the Yamal Peninsula, in the Pyasinsky Bay and the waters of the Nordenskiöld Archipelago (Fig. 3). Thus, polygon $Q_{p=1}$ consists of three or four isolated regions. The polygon of the probability of detecting landfast ice is interrupted at the exits from the Gulf of Ob and the Yenisei Bay, as well as in the area of the Cape of Dickson. For all 22 years, in the first ten days of May, landfast ice has always been observed near the islands of Sergei Kirov, Voronin Island, and in the straits of the Severnaya Zemlya Archipelago.

The area, where landfast ice is observed at least once in the first ten days of May (the maximum possible development of landfast ice) is a vast polygon $Q_{p=1/22}$ connected to the mainland and including all the islands of the considered part of the Kara Sea, except for Uedineniya Island. The edges of the polygon $Q_{p=1/22}$ are located approximately 20 km north of the Izvestiya TSIK, Sergei Kirov, and Voronin islands. The distance from the islands of Izvestiya TSIK and Arctic Institute to the edge of the polygon $Q_{p=1/22}$ is about 10 km. The edge of the polygon $Q_{p=1/22}$ is located at a distance of 30 to 60 km from Vilkitsky, Shokalsky, and Belyi islands. The polygon $Q_{p=1/22}$ near the Yamal Peninsula is 30–50 km wide; near the Vaigach and Yugorsky peninsulas, its width is approximately 10 km. Uedineniya Island has a separate landfast ice (the maximum width of the landfast ice is up to 20 km). In addition, there are local areas of landfast ice isolated from the shore, which in shallow water areas can form for a short time near ice hummocks. It should also be recognized that in some cases the drifting fields of detached landfast ice on the electronic ice charts of the AARI are also designated as landfast ice.

The region of landfast ice occurrence with a probability of 0.5 is divided into three parts: landfast ice near Vaigach Island and the northern part of the Yugor Peninsula; landfast ice along the Baidaratskaya Bay, Yamal, Gulf of Ob, Gydan Bay, and Yenisei Bay shores; and landfast ice to the west of the Dikson Island along the coast of the Taimyr Peninsula and the Severnaya Zemlya Archipelago. Inside the polygon $Q_{p=0.5}$ connected to the mainland, there are the islands of Belyi, Shokalsky, Vilkitsky, Sergei Kirov, and Voronin. Isolated median polygons of landfast ice occurrence are noted near the islands of Sverdrup, Arctic Institute, Izvestiya TSIK, and Uedineniya. A part of the coast near Dikson Island is not included in the polygon $Q_{p=0.5}$; in more than 50% of cases, landfast ice is not observed in this part of the sea.

The dotted line in Fig. 3 shows the lines of the polygons of probabilities 0.25 and 0.75, obtained by two-dimensional interpolation of the coordinates of the polygon vertices. In the space between these two polygons, the landfast ice edge will be located in 50% of cases.

The distance between polygons of quartiles is called interquartile distance Q_{IQR}. As we can see from Fig. 3, the polygon of interquartile distance has a different length in different parts of the sea: in Baydaratskaya Bay and off the western coast of the Yamal Peninsula, its width is about 10 km; to the east of Be-

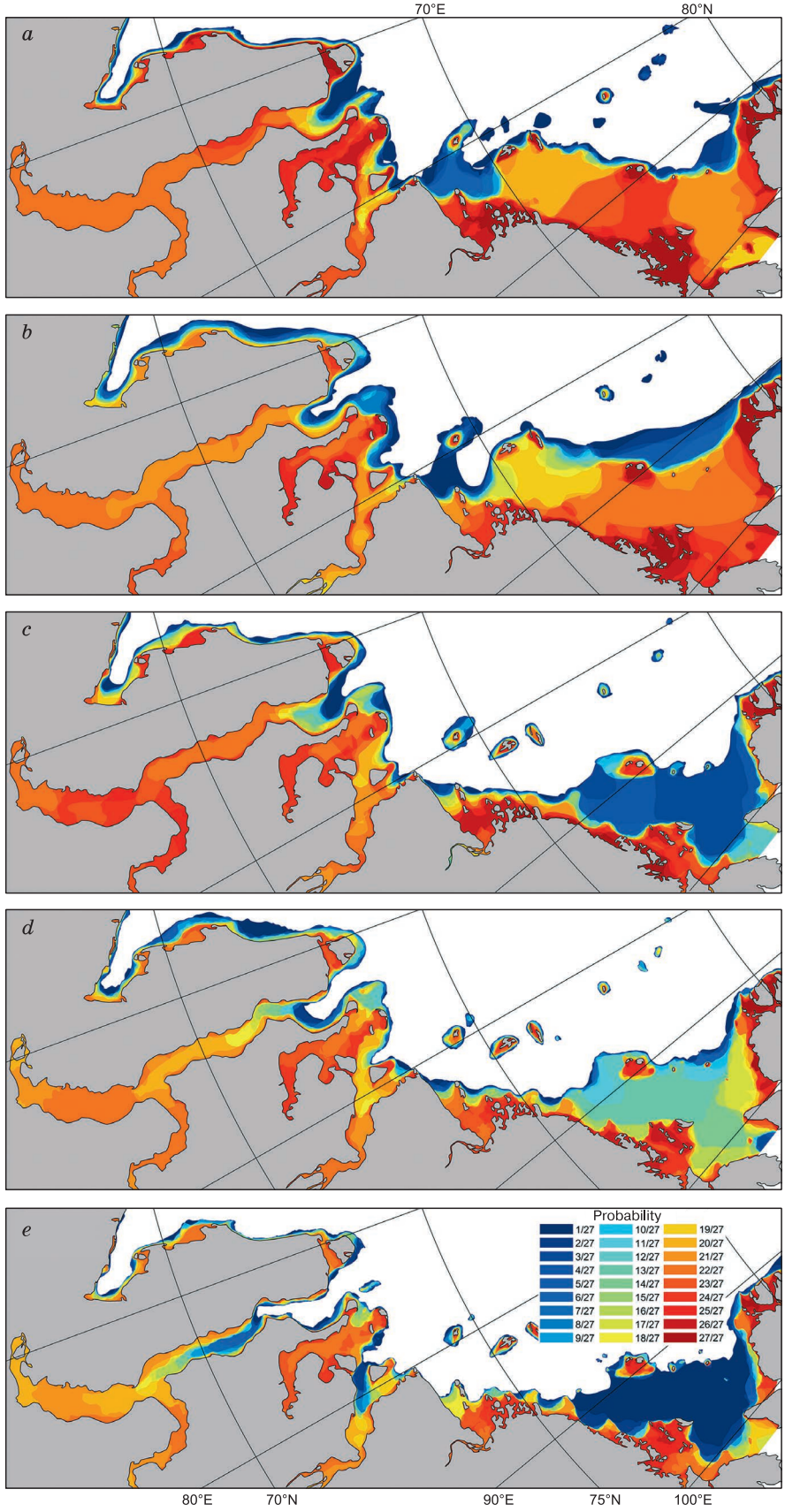

Fig. 2. The probability of finding landfast ice from November 1 to July 31 in different years:

(*a*) November 1999–July 2000; (*b*) November 2004–July 2005; (*c*) November 2009–July 2010; (*d*) November 2014–July 2015; (*e*) November 2019–July 2020.

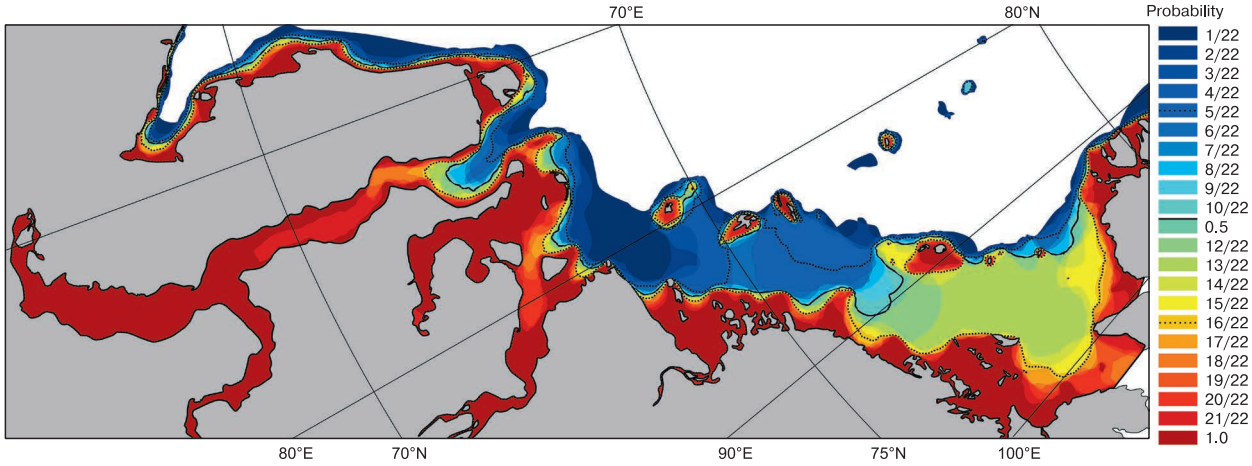

Fig. 3. Probability of landfast ice occurrence in the first ten days of May (1998–2020).

lyi Island at the entrance to the Gulf of Ob, the width of the Q_{IQR} polygon is 20 km; the maximum width (90 km) is in the Gulf of Ob itself. In the water area between the islands of the Arctic Institute and Sergey Kirov, the polygon of interquartile distance has a width of 50–100 km; to the east of the 90° E meridian, the width of the Q_{IQR} polygon increases to 100–200 km. Figure 3 shows that the islands of the Arctic Institute, Sergey Kirov, and Voronin are located inside the $Q_{p=0.25}$ quartile polygon connected to the mainland coast. The islands of Sverdrup, Izvestiya TSIK, and Uedineniya have their own isolated polygons of the quartile $Q_{p=0.25}$.

It can be seen that the faces of the interquartile polygons $Q_{p=0.25}$ and $Q_{p=0.75}$ are located asymmetrically relative to the line of the median polygon $Q_{p=0.5}$ (Fig. 3), which indicates an asymmetric distribution of the probabilities of landfast ice occurrence along the directions orthogonal to the shore and the probability polygons Q_p. Moreover, the asymmetry of the distribution changes sign: east of the 90° E meridian, the distance between polygon faces $Q_{p=0.75}$ and $Q_{p=0.5}$ is greater than the distance between polygons $Q_{p=0.25}$ and $Q_{p=0.5}$. At the entrance to the Gulf of Ob and in the water area located between the islands of the Arctic Institute and the islands of Sergei Kirov, an opposite trend is noted.

The position of the isolines of the probability of landfast ice occurrence shown in Figs. 2 and 3 are consistent with the known regime characteristics of the Kara Sea. Air temperature, bottom relief, configuration of coasts and islands, and wind and hydrological regimes determine the development of landfast ice [*Gordienko, 1971; Gudkovich et al., 1972; Gorbunov et al., 1983; Karelin, Karklin, 2012*]. The formation of landfast ice occurs after the onset of ice formation in the coastal part when young ice reaches the gray-white stage (thickness range 20–30 cm). At the beginning of the winter period, an intensive increase in the width of the landfast ice takes place, which is associated with an increase in the thickness of the ice and the strengthening of the ice plate itself. In the middle of winter, the development of landfast ice width slows down and stops altogether. The width of landfast ice can change as a result of the action of offshore or pressure winds, and periodic and surge fluctuations in sea level. In spring, due to the above-zero temperature and the flow of solar radiation, the ice begins to melt and collapse. The strength of the ice cover is significantly reduced and an abrupt decrease

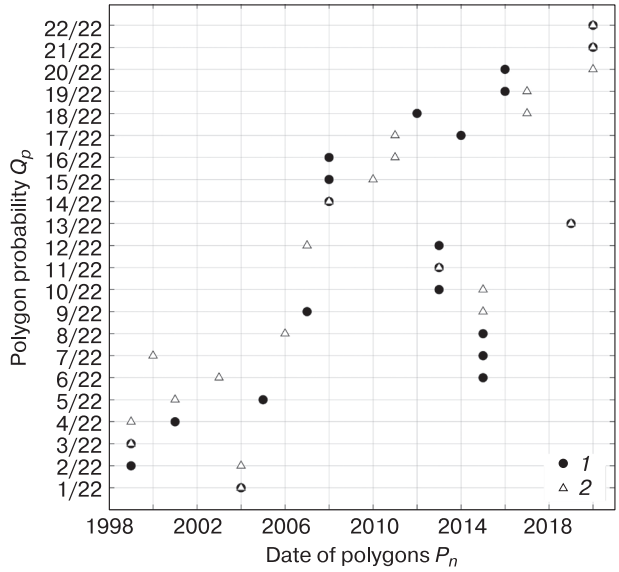

Fig. 4. Correspondence of polygons of probabilities Q_p and landfast ice polygons P_n in the first ten days of May (1998–2020) calculated as:

(*1*) minimum area of polygons $(Q_p \backslash P_n) \cup (P_n \backslash Q_p)$; (*2*) minimum difference between polygon areas Q_p and P_n.

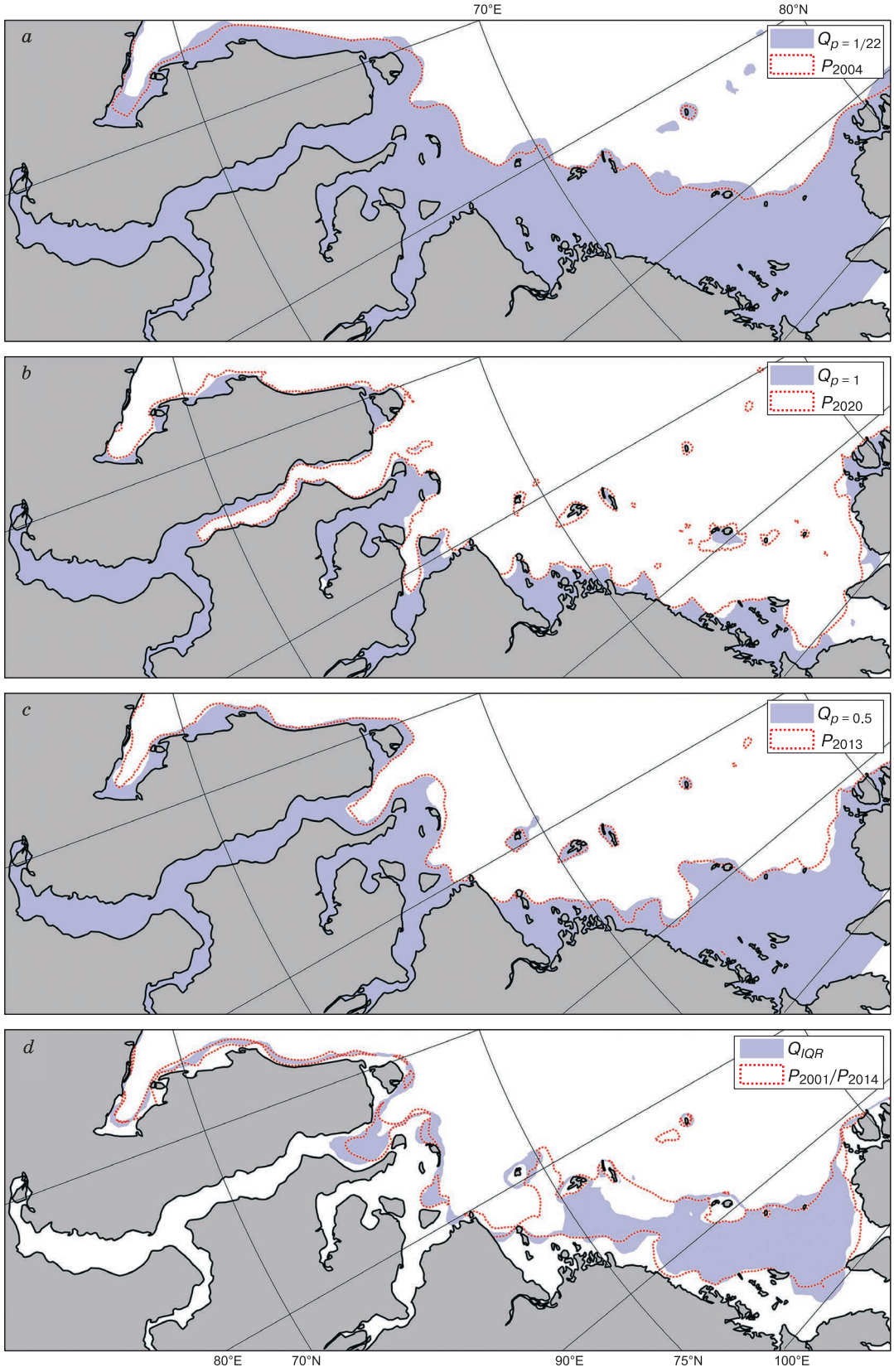

Fig. 5. Areas of landfast ice occurrence in the first ten days of May with a probability of:
(*a*) 1/22, (*b*) 1, (*c*) 0.5; (*d*) area of interquartile distance.

in the landfast ice width is observed; its pattern depends on the direction and strength of the wind. Breaking up of landfast ice, as a rule, starts from its seaward edge and moves towards the coast, although cases of rapid complete destruction of the entire landfast ice were sometimes noted.

Such a scheme of landfast ice dynamics determines the maximum probabilities of detecting landfast ice near the shore. Noted in Fig. 2, the trend of landfast ice area reduction is consistent with the general positive trend of air temperature changes in this area [*Karelin, Karklin, 2012*].

The resulting polygons of landfast ice detection probabilities Q_p are a complex combination of the results of combining and crossing different landfast ice fragments P_n measured from satellite images in different years. In some cases, it is required to select an analogue of the polygon of the probability of detecting landfast ice Q_p from the array of measured landfast ice boundaries in different years. Polygons-analogues were selected according to two criteria: (1) minimum area of the symmetric difference $(Q_p \setminus P_n) \cup (P_n \setminus Q_p)$ and (2) minimum difference between the areas of polygons Q_p and P_n (Fig. 4). Figure 4 shows the correspondence between the probability polygons Q_p and the landfast ice polygons P_n for the first ten days of May. There is a unidirectional trend here: in that period, polygons with high probability values of landfast ice occurrence correspond to landfast ice polygons of recent years (2014–2020); larger polygons with low probabilities correspond to landfast ice polygons surveyed in the first half of the period under consideration (1998–2008). The noted trend also indicates a decrease in landfast ice area over the past 22 years.

The polygon of the probability of finding landfast ice $Q_{p=1/22}$ should be greater than or equal to the largest landfast ice of all marked on satellite images. Therefore, for the polygon $Q_{p=1/22}$, both criteria indicated the presence of landfast ice on May 5, 2004 (Fig. 5*a*). A similar situation develops with the polygon minimally possible in terms of area $Q_{p=1}$, showing the area where landfast ice at the beginning of May was recorded during the entire period (22 years) of observation. Both criteria pointed to the last of the AARI ice charts under consideration dated May 5, 2020 (Fig. 5*b*). The median line of the landfast ice appearance (polygon $Q_{p=0.5}$) best coincides with the landfast ice recorded on May 7, 2013 (Fig. 5*c*). In other cases, the selection criteria under consideration give, as a rule, different results, and according to the criterion $(Q_p \setminus P_n) \cup (P_n \setminus Q_p)$, a more accurate coincidence of the faces of the polygons Q_p and P_n is noted. The area of interquartile distance Q_{IQR} is limited by polygons $Q_{p=0.25}$ and $Q_{p=0.75}$; landfast ice edge lines for May 7, 2014, and May 8, 2001, can be used as their analogues, respectively (Fig. 5*d*).

CONCLUSIONS

The parameters of the natural environment are n-dimensional functions ($n \geqslant 1$), which are recorded during observations as a discrete data set in n-dimensional space. With the development of numerical methods and computational technologies, there is an increasing demand to obtain and analyze data in their original form, i.e., in the form of continuous n-dimensional functions, without simplifying discretization. Thus, in recent decades, a separate direction in mathematical statistics has been distinguished – the analysis of functional data [*Ramsay, Silverman, 2005*]. This analysis, based on the use of raw data, finds application in various fields of science, including the earth sciences.

Obviously, such an analysis is also in demand in the study of the ice cover. There are several prerequisites for this: (a) in nature, the edge of drifting ice, landfast ice, and polynyas is a closed line; (b) traditionally spatially distributed ice information is summarized and recorded in the form of ice zones, which are also closed lines; (c) electronic ice charts adopted by the World Meteorological Organization are not raster images, but sets of vector polygons designed as shape-files with geoinformation reference.

In the present work, apparently, the first attempt has been made to apply the initial vector data to the analysis of information on the spatial distribution of the ice cover. Based on standard, strictly formalized and optimally implemented operations with vector polygons in many applied software libraries, algorithms for calculating the probabilities of crossing polygons were developed, with the help of which the probability (repeatability) of finding landfast ice in the Kara Sea was calculated. Formally, the method proposed by the authors cannot be classified as a method of analysis of functional data. However, it is based on the same ideology of eliminating intermediate procedures associated with the transfer of functions (polygons) into a set of discrete values (matrices or a set of sections).

The proposed method was applied to assess the probability of occurrence of landfast ice in the Kara Sea for the period from 1998 to 2020. The area of extreme distribution of landfast ice in the first ten days of May includes the islands of Vilkitsky, Shokalsky, Belyi, the Arctic Institute, Izvestiya TSIK, Sergey Kirov, and Voronin. The edge of this area is located 10–20 km north of the Izvestiya TSIK, Sergey Kirov, and Voronin islands and 30 to 60 km north of the Vilkitsky, Shokalsky, and Bely islands.

An analysis of the variability of landfast ice edge coordinates over different years showed that over the considered period of 22 years, there was a decrease in the area of landfast ice. This conclusion was confirmed both by comparing the interannual variability of the frequency of landfast ice position during the cold sea-

son and by fitting the measured polygons to different polygons of the probability of landfast ice occurrence. Landfast ice in 1998–2008 corresponds, as a rule, to polygons with the minimum probability and maximum areas, and, conversely, the landfast ice observed in May 2020 generally corresponds to the area, where landfast ice is always observed, i.e., to the polygon with the maximum probability and minimum area.

This algorithm can be applied to estimate the probability of occurrence of any data represented as polygonal features. Such objects are used in many Earth sciences, including hydrometeorology and glaciology, for example, to describe ice edges, glacier boundaries, permafrost, snow cover, and the position of certain field boundaries (isotherms, isobars, etc.). Thus, the potential scope of the proposed methodology can be much wider than the examples discussed in the article.

Acknowledgments. *This study was supported by the Russian Science Foundation, project no. 17-79-20162.*

References

Arkhipov V.V., Kokin O.V., Ogorodov S.A. et al., 2017. Landfast ice edge near the Yamal coast of the Baydaratskaya Bay of the Kara Sea in 2012–2016: its dynamics and role in the formation of modern furrows on the seabed. *Vesti gazovoy nauki* **4** (32), 129–136 (in Russian).

Atlas of Ice Formations, 2018. V.M. Smolyanitskiy (ed.). St. Petersburg, AARI, 230 pp. (in Russian).

Afanasyeva E.V., Alekseeva T.A., Sokolova Yu.V. et al., 2019. AARI methodology for sea ice charts composition. *Rossiiskaya Arktika* **7**, 5–20 (in Russian).

Divine D.V., Korsnes R., Makshtas A.P., 2004. Temporal and spatial variation of shore-landfast ice in the Kara Sea. *Continental Shelf Res.* **24** (15), 1717–1736.

Dmitrenko I.A., Gribanov V.A., Volkov D.L. et al., 1999. Impact of river discharge on the landfast ice extension in the Russian Arctic shelf area. In: *Proc. of the 15th Int. Conf. on Port and Ocean Engineering under Arctic Conditions (POAC99)* (Helsinki, August 23–27, 1999). Helsinki, Finland, 1999, pp. 311–321.

Galley R.J., Else B.G.T., Howell S.E.L. et al., 2012. Landfast sea ice conditions in the Canadian Arctic: 1983–2009. *Arctic* **65** (2), 133–144.

Gorbunov Yu.A., Karelin I.D., Kuznetsov I.M. et al., 1983. *Fundamentals of Physical and Statistical Methods of Ice Forecasting and Calculations for the Arctic Seas with a Lead Time of up to 30 Days*. Leningrad, Gidrometeoizdat, 288 pp. (in Russian).

Gordienko P.A., 1971. *Landfast ice of the Arctic seas. Parts I–II*. Leningrad, Gidrometeoizdat, 172 pp. (in Russian).

Gudkovich Z.M., Kirillov A.A., Kovalev K.G. et al., 1972. *Fundamentals of the Methodology for Long-term Ice Forecasting for the Arctic Seas*. Leningrad, Gidrometeoizdat, 348 pp. (in Russian).

Karelin I.D., Karklin V.P., 2012. *Landfast ice and Polynyas of the Arctic Seas of the Siberian Shelf in the Late XX–Early XXI century*. St. Petersburg, Izd. AARI, 180 pp. (in Russian).

Li Z., Zhao J., Su J. et al., 2020. Spatial and temporal variations in the extent and thickness of Arctic landfast ice. *Remote Sensing* **12**, 64.

Lopez-Pintado S., Romo J., 2009. On the concept of depth for functional data. *J. Amer. Statistical Assoc.* **104** (486), 718–734.

Mahoney A.R., Eicken H., Gaylord A.G., Gens R., 2014. Landfast sea ice extent in the Chukchi and Beaufort Seas: The annual cycle and decadal variability. *Cold Regions Sci. and Technol.* **103**, 41–56.

Mahoney A.R., Eicken H., Gaylord A.G., Shapiro L., 2007. Alaska landfast sea ice: Links with bathymetry and atmospheric circulation. *J. Geophys. Res.* **112** (C2), C02001.

Pavlova E.A., May R.I., Mironov E.U. et al., 2019. Methods of calculating the statistical parameters of landfast ice edge distribution. In: *Proc. of the III All-Russian Conf. Hydrometeorology and Ecology: Achievements and Development Prospects"* (St. Petersburg, Dec. 18–19, 2019). St. Petersburg, Khimizdat, pp. 669–672 (in Russian).

Ramsay J.O., Silverman B.W., 2005. *Functional Data Analysis*. New York, Springer Verlag, 429 pp.

Selyuzhenok V., Krumpen T., Mahoney A. et al., 2015. Seasonal and interannual variability of landfast ice extent in the southeastern Laptev Sea between 1999 and 2013. *J. Geophys. Res. Oceans* **120**, 7791–7806.

URL: http://wdc.aari.ru/datasets (last visited: Sept. 1, 2022).

URL: https://www.mathworks.com/matlabcentral/fileexchange/99879-probability-of-polygons-intersection (last visited: Sept. 1, 2022).

Vize V.Y., 1944. *The Foundations of Long-Range Ice Forecasting for the Arctic Seas*. Moscow, Izd. Glavsevmorputi, 272 pp. (in Russian).

Vize V.Y., 1948. *Seas of the Soviet Arctic*. Moscow, Leningrad, Izd. Glavsevmorputi, 416 pp. (in Russian).

Volkov N.A. (ed.), 1981. *Guide to the Production of Ice Air Surveys*. Leningrad, Gidrometizdat, 239 pp. (in Russian).

WMO No. 259, 2014. *The WMO Sea Ice Nomenclature. Vol. 1. Terminology and Codes*. WMO, JCOMM Expert Team on Sea Ice, 121 pp.

Yu Y., Stern H., Fowler C. et al., 2014. Interannual variability of Arctic landfast ice between 1976 and 2007. *J. Climate* **27**, 227–243.

Zubov N.N., 1944. *Arctic Ice*. Moscow, Izd. Glavsevmorputi, 360 pp. (in Russian).

Received September 28, 2021
Revised April 9, 2022
Accepted September 14, 2022

Translated by A.V. Muravyev